

In Situ Detection of Programmed Cell Death Protein 1 and Programmed Death Ligand 1 Interactions as a Functional Predictor for Response to Immune Checkpoint Inhibition in NSCLC



Amanda Lindberg, MSc,^a Lars Muhl, PhD,^{b,c} Hui Yu, MSc,^a Louise Hellberg, BSc,^a Rebecca Artursson, MSc,^a Jakob Friedrich, MD,^a Max Backman, MD, PhD,^a Neda Hekmati, MSc,^a Johanna Mattsson, PhD,^a Cecilia Lindskog, PhD,^a Hans Brunnström, MD, PhD,^d Johan Botling, MD, PhD,^{a,e} Artur Mezheyeuski, MD, PhD,^{f,g} Erika Broström, MD,^{a,h} Miklos Gulyas, MD, PhD,^a Klas Kärre, MD, PhD,ⁱ Johan Isaksson, MD, PhD,^a Patrick Micke, MD, PhD,^a Carina Strell, PhD^{a,c,*}

^dDivision of Pathology, Lund University, Lund, Sweden

Received 23 September 2024; revised 6 December 2024; accepted 27 December 2024 Available online - 30 December 2024

ABSTRACT

Introduction: Immune checkpoint inhibitors (ICIs) have transformed lung cancer treatment, yet their effectiveness seem restricted to certain patient subsets. Current clinical stratification on the basis of programmed death ligand 1 (PD-L1) expression offers limited predictive value. Given the mechanism of action, directly detecting spatial programmed cell death protein 1 (PD1)–PD-L1 interactions might yield more precise insights into immune responses and treatment outcomes.

Methods: We applied a second-generation in situ proximity ligation assay to detect PD1-PD-L1 interactions in diagnostic tissue samples from 16 different cancer types, a tissue microarray with surgically resected early-stage NSCLC, and finally diagnostic biopsies from 140 patients with advanced NSCLC with and without ICI treatment. RNA sequencing analysis was used to identify potential resistance mechanisms.

Results: In the early-stage NSCLC, only approximately half of the cases with detectable PD-L1 and PD1 expression exhibited PD1-PD-L1 interactions, with significantly lower levels in EGFR-mutated tumors. Interaction levels varied

across cancer types, aligning with reported ICI response rates. In ICI-treated patients with NSCLC, higher PD1-PD-L1 interactions were linked to complete responses and longer survival, outperforming standard PD-L1 expression assays. Patients who did not respond to ICIs despite high PD1-PD-L1 interactions exhibited additional expression of stromal immune mediators (*EOMES, HAVCR1*/TIM-1, *IAML, FCRL1*).

*Corresponding author.

Drs. Micke and Strell contributed equally to this work as co-senior authors.

Address for correspondence: Carina Strell, PhD, Department of Immunology, Genetics, and Pathology, Uppsala University, Rudbecklaboratoriet, Dag Hammarskjölds väg 20, 751 85 Uppsala, Sweden. E-mail: carina.strell@igp.uu.se

Cite this article as: Lindberg A, Muhl L, Yu H, et al. In situ detection of programmed cell death protein 1 and programmed death ligand 1 interactions as a functional predictor for response to immune checkpoint inhibition in NSCLC. *J Thorac Oncol*. 2025;20:625-640.

© 2025 International Association for the Study of Lung Cancer. Published by Elsevier Inc. This is an open access article under the CC BY license (http://creativecommons.org/licenses/by/4.0/).

ISSN: 1556-0864

https://doi.org/10.1016/j.jtho.2024.12.026

^aDepartment of Immunology, Genetics, and Pathology, Uppsala University, Uppsala, Sweden

^bDepartment of Medicine (Huddinge), Karolinska Institutet, Huddinge, Sweden

^cCentre of Cancer Biomarkers (CCBIO), Department of Clinical Medicine, University of Bergen, Bergen, Norway

^eDepartment of Laboratory Medicine, Institute of Biomedicine, Sahlgrenska Academy, University of Gothenburg, Gothenburg, Sweden

^fVall d'Hebron Institute of Oncology, Molecular Oncology Group, Barcelona, Spain

^gVall d'Hebron Institute of Research, Barcelona, Spain

^hDepartment of Medical Sciences, Uppsala University, Uppsala, Sweden

ⁱDepartment of Microbiology, Cell and Tumor Biology, Karolinska Institutet, Stockholm, Sweden

Conclusion: Our study proposes a diagnostic shift from static biomarker quantification to assessing active immune pathways, providing more precise ICI treatment. This functional concept applies to tiny lung biopsies and can be extended to further immune checkpoints. Accordingly, our results indicate concerted ICI resistance mechanisms, highlighting the need for combination diagnostics and therapies.

© 2025 International Association for the Study of Lung Cancer. Published by Elsevier Inc. This is an open access article under the CC BY license (http://creativecommons.org/licenses/by/4.0/).

Keywords: Immune checkpoint inhibitor; Programmed death ligand 1; Programmed cell death protein 1; non-small cell lung cancer; Proximity ligation assay

Introduction

The introduction of immune checkpoint inhibitors (ICIs) has revolutionized cancer therapy in many tumor types. ICIs block the interaction of co-inhibitory receptors expressed on T cells or natural killer cells (e.g., programmed cell death protein 1 [PD1]) with their corresponding ligands on tumor cells or antigen-presenting cells (e.g., programmed death ligand 1 [PD-L1]), thereby unleashing a strong reactivation of antitumor immune responses. Several ICIs targeting the PD1/PD-L1 axis are now approved by the U.S Food and Drug Administration and the European Medicines Agency for advanced NSCLC, including anti-PD1 (e.g., nivolumab, pembrolizumab) and anti-PD-L1 (e.g., atezolizumab, durvalumab) antibodies. However, their efficacy varies substantially among patients, with only a minor subset exhibiting a durable response.²⁻⁶ Although ICIs are better tolerated than chemotherapy, serious and sometimes fatal immune-related adverse events occur, highlighting the need to carefully select patients who will experience true benefit from this therapy option.

Today, patient stratification for anti-PD1/anti-PD-L1 ICI therapies is based on the proportion of tumor cells showing membranous PD-L1 expression, the so-called tumor proportion score (TPS). Several diagnostic assays are used to perform this immunohistochemical analysis on diagnostic biopsies of patients with NSCLC. In lung cancer, TPS cutoffs for PD-L1 of greater than or equal to 1% and greater than or equal to 50% are relevant for the choice of ICI therapy⁸; however, their value to predict ICI treatment benefit is only modest as many patients with NSCLC having a high PD-L1 TPS are not responding to ICI therapies, whereas some responders are observed among PD-L1 low cases, resulting in substantial over- and undertreatment. PD-L2 Evidently, PD-

L1 protein expression is insufficient to explain the biologic mechanism and subsequent clinical effects of ICIs' anticancer immune responses.

Conceptually, immune inhibitory signaling means of PD1 requires direct interaction with one of its ligands, for instance, PD-L1. This interaction is the ultimate target of ICI therapies with antibodies against PD1 or PD-L1. As the interaction of PD1 with PD-L1 is the definite regulatory mechanism, it should also be a better clinical predictor for ICI efficacy than PD-L1 protein quantification alone. Two previous studies have provided supporting evidence for this concept using two different spatial approaches. A high colocalization score of PD1 and PD-L1 as assessed by means of multiplexed quantitative immunofluorescence, or interaction by means of Förster resonance energy transfer, was associated with longer survival in ICI-treated NSCLC cohorts. 13,14 These findings motivate a paradigm shift, from single PD-L1 quantification toward a metric of active PD1-PD-L1 signaling, which holds the promise to better stratify patients for ICI treatment benefit. However, advanced spatial analyses of interactions are challenging, particularly with regard to an introduction into routine diagnostic pipelines.

The proximity ligation assay (PLA) technique offers an elegant alternative to identify protein-protein interactions in the in situ microenvironment of tissues. Since its first introduction, further development into a second-generation PLA utilizing antibodies conjugated to unfold probes, which are enzymatically unfolded only after the antibodies have bound their corresponding targets, reduced nonspecific background. 15 More importantly, the PLA is applicable to formalin-fixed paraffin-embedded (FFPE) tissue samples, a prerequisite for any diagnostic assay. The PLA technique does not require advanced imaging appliances but can be simply performed as a robust brightfield assay, which can be analyzed by manual pathologic evaluation or with tools already available today in many pathology departments, allowing for easy integration into clinical diagnostic routines.

In this study, we sought to map PD1-PD-L1 interactions in diagnostic NSCLC biopsies, assessing their predictive value for ICI treatment. PD1-PD-L1 interactions were mainly found in the stromal compartment and, more importantly, patients with higher levels were strongly associated with complete responses and longer survival under ICI therapy. Of note, the standard PD-L1 TPS did not effectively distinguish patients who benefited from ICI therapies. RNA sequencing (RNA-seq) analysis revealed that nonresponders with high PD1-PD-L1 levels had elevated expression of additional stromal immune mediators, suggesting resistance mechanisms.

Methods

Patient Materials

The Uppsala I training cohort consists of 352 patients with NSCLC surgically treated at Uppsala University Hospital, Sweden, between 1995 and 2005 (ethical permit Dnr2006/325), constructed into tissue microarrays (TMAs), as described previously.¹⁶

A pancancer TMA consisting of 16 different solid tumor types was constructed with two cores representing each patient (ethical permit Ups02-577 and Dnr2011/473).

The Sjöberg ICI cohort includes patients with NSCLC treated at Uppsala University Hospital with ICI therapies in various treatment lines and modalities (Table 1). The retrospective inclusion of patients for cohort collection started in 2016 (ethical permit Dnr2017/076 and Dnr2023/07131-02, including informed consent) and is still ongoing; clinical database status as of July 2024 was used. For the presented study, the predefined time frame of inclusion was from 2015 to 2022, resulting originally in 133 patients with NSCLC. The second inclusion criterion was having received multiple ICI cycles at the time of the study end point. A matched NSCLC control cohort was collected including 109 patients with NSCLC who had not received ICI treatment regimens but received other standard-of-care therapies (Table 1). All patients had undergone pretreatment diagnostic biopsies. Paraffin blocks of the remaining tumor biopsies after diagnostic evaluation could be retrieved for 72 ICI-treated patients and 78 ICI treatment-naive patients and were sectioned at 4-mm thickness. After pathologic assessment (PM), 67 and 73 samples from each cohort, respectively, had viable tissue for the analysis of PD1-PD-L1 interaction (Supplementary Fig. 1, CONSORT diagram).

This study was conducted in accordance with the Declaration of Helsinki and the Swedish Ethical Review Act.

Immunohistochemistry

Immunohistochemistry (IHC) for PD-L1, PD1, CD4, and CD20 (antibody details in Supplementary Table 1) was performed on a Bond RXm autostainer (Leica Biosystems; Nussloch, Germany) using Dewax solution for deparaffinization (#AR9222, Leica Biosystems) followed by an antigen retrieval step with either Epitope Retrieval solution 1 or 2 (#AR9961 or #AR9640, respectively) at 100°C for 30 minutes. The Bond Polymer Refine Detection kit (#DS9800) and Haematoxylin II as a counterstain were used according to the manufacturer's instructions. All slides were dehydrated before mounting with VectaMount Permanent Mounting Medium (#H-5000, Vector Laboratories, Newark, NJ). The slides were scanned using the VectraPolaris system (Akoya Biosciences, Marlborough, MA) at a resolution of 0.5 mm/

pixel. Other mentioned immune markers had been stained previously and are described in Supplementary Table 1 and in detail elsewhere. 17,18

PLA: Identification of PD1-PD-L1 Interactions

The Naveni PD1/PD-L1 AP (#NPT.PD-L1.AP.100, Navinci Diagnostics, Uppsala, Sweden) PLA kit was used to detect the PD1-PD-L1 interaction in tissue samples. Initial deparaffinization and antigen retrieval with Epitope Retrieval solution 2 were performed on the Bond RXm autostainer (Leica Biosystems). PLA was carried out according to the manufacturer's instructions. The slides were scanned using the VectraPolaris system (Akoya Biosciences) at a resolution of 0.5 mm/pixel.

Manual Annotation of Expression and Interaction Patterns

Manual annotations of IHC and PLA staining were scored as a percentage of positive cells within the whole tissue and separately for the stromal and tumor compartments (according to the following increments: 0 = <1%, 1 = 1%-4%, 5 = 5%-9%, 10 = 10%-14%, 15 = 15%-19%, 20 = 20%-24%, 25 = 25%-29%, 30 = 30%-34%, 35 = 35%-39%, 40 = 40%-44%, 45 = 45%-49%, 50 = 50%-59%, 60 = 60%-69%, 70 = 70%-79%, 80 = 80%-89%, $90 = \geq 90\%$). For the Uppsala I training cohort, annotations of PLA and PD1 IHC (AL), CD4 IHC (LH), and PD-L1 and CD20 IHC (MB, clone SP142-certified pathologist) were performed. Scores from TMA cores representing the same patient were averaged.

The Sjöberg cohort was annotated (PM, board-certified lung pathologist) with regard to their PLA pattern. Here, additional increments of 0 = 0%, and 0% to 1% positivity were added for a more in-depth scoring. To evaluate the reproducibility of the pathologic annotations, the cohort was independently assessed by a separate rater (AL). Previously reported PD-L1 expression levels as investigated by means of IHC (clone 22C3, Agilent Dako) for diagnostic purposes were retrieved from patients' clinical records.

Automated Annotation Pipeline for the Detection of Positive Cells in QuPath

QuPath (version 0.5.0¹⁹) was used for automated digital staining annotations. Default convolution settings were used for the Haematoxylin stain vector; the FastRed channel's red, green and blue values were set to 0.121, 0.851, and 0.510, whereas the residual channel's red, green and blue values were set to 0.495, 0.592, and 0.636. Initially, manual image curation was performed to exclude necrosis, staining artifacts, lumens, and other empty spaces. Furthermore, cell detection was

Table 1. Patient Characteristics

Uppsala ICI treatment cohort

	All patients n = 140			ICI-treated patients $n=67$			ICI-naive/control n = 73		
Variable	ICI-treated n = 67 (47.9)	ICI-naive/control n = 73 (52.1)	p Value	Low PD1-PD-L1 n = 36 (53.7)	High PD1-PD-L1 n = 31 (46.3)	p Value	Low PD1-PD-L1 n = 63 (86.3)	High PD1-PD-L1 n = 10 (13.7)	p Value
Histological subtype:									
SqCC	21 (31.3)	15 (20.5)	0.004	12 (33.3)	9 (29.0)	0.18	14 (22.2)	1 (10.0)	0.68
AC	40 (59.7)	58 (79.5)		23 (63.9)	17 (54.9)		49 (77.8)	9 (90.0)	
Other	6 (9.0)	0 (0.0)		1 (2.8)	5 (16.1)		0 (0.0)	0 (0.0)	
Diagnostic TPS - PD-L1 ^a :									
<1%	17 (27.4)	6 (15.8)	0.23	11 (32.4)	6 (21.4)	0.40	5 (16.1)	1 (14.3)	1.00
≥1%	45 (72.6)	32 (84.2)		23 (67.6)	22 (78.6)		26 (83.9)	6 (85.7)	
Diagnostic TPS - PD-L1a:									
<50%	35 (56.5)	26 (68.4)	0.29	24 (70.6)	11 (39.3)	0.020	23 (74.2)	3 (42.9)	0.18
≥50%	27 (43.5)	12 (31.6)		10 (29.4)	17 (60.7)		8 (25.8)	4 (57.1)	
Stage ^b :									
1-111	16 (23.9)	36 (49.3)	0.003	10 (27.8)	6 (19.4)	0.57	32 (50.8)	4 (40.0)	0.74
IV	51 (76.1)	37 (50.7)		26 (72.2)	25 (80.6)		31 (49.2)	6 (60.0)	
Age at diagnosis:									
<70 years	36 (53.7)	27 (37.0)	0.061	22 (61.1)	14 (45.2)	0.23	24 (38.1)	3 (30.0)	0.74
≥70 years	31 (46.3)	46 (63.0)		14 (38.9)	17 (54.8)		39 (61.9)	7 (70.0)	
Sex:	,	, ,		` '	,		,	, ,	
Male	35 (52.2)	36 (49.3)	0.74	21 (58.3)	14 (45.2)	0.33	32 (50.8)	4 (40.0)	0.74
Female	32 (47.8)	37 (50.7)		15 (41.7)	17 (54.8)		31 (49.2)	6 (60.0)	
Smoking:	, ,	, ,		, ,	, ,		, ,	,	
Never-smoker	8 (11.9)	11 (15.1)	0.63	5 (13.9)	3 (9.7)	0.72	10 (15.9)	1 (10.0)	1.00
Current/former smoker	59 (88.1)	62 (84.9)		31 (86.1)	28 (90.3)		53 (84.1)	9 (90.0)	
Performance status ^c :	, ,	, ,		, ,	, ,		, ,	, ,	
0	20 (29.9)	24 (33.8)	0.41	14 (38.9)	6 (19.4)	0.093	21 (33.9)	3 (33.3)	0.40
1	34 (50.7)	28 (39.4)		14 (38.9)	20 (64.5)		26 (41.9)	2 (22.2)	
2-4	13 (19.4)	19 (26.8)		8 (22.2)	5 (16.1)		15 (24.2)	4 (44.4)	
Principal therapy ICI-trea	ted patients:	, ,		, ,	, ,		,	, ,	
Nivolumab	22 (32.8)		na	13 (36.1)	9 (29.0)	0.71		-	-
Pembrolizumab	30 (44.8)	-		14 (38.9)	16 (51.6)			-	
Atezolizumab	9 (13.4)			6 (16.7)	3 (9.7)			-	
Other/ICI combinations	6 (9.0)	-		3 (8.3)	3 (9.7)			-	
Anti-PD1/-PD-L1 therapy	` '			(()	, ,				
monotherapy	50 (74.6)	-	na	28 (77.8)	22 (71.0)	0.58	-		-
+ chemo/other ICI	17 (25.4)			8 (22.2)	9 (29.0)			-	
ICI treatment line ^d :	(==: ')			- \/	. (=::-/				
1	33 (50)		na	15 (41.7)	18 (60.0)	0.22		-	
≥2	33 (50)		114	21 (58.3)	12 (40.0)	V.22			
	55 (50)			2. (55.5)	(10.0)				

(continued)

Table 1. Continued Uppsala ICI treatment cohort

	All patients $n=140$	140		ICI-treated patients $n=67$	ts n = 67		ICI-naive/control n = 73	n=73	
Variable	ICI-treated n = 67 (47.9)	ICI-naive/control n = 73 (52.1)	p Value	Low PD1-PD-L1 n = $36 (53.7)$	High PD1-PD-L1 $n = 31 (46.3)$	p Value	Low PD1-PD-L1 n = 63 (86.3)	High PD1-PD-L1 $n = 10 (13.7)$	p Value
Therapy ICI-naive patients:									
Chemotherapy		35 (47.9)	na				31 (49.2)	4 (40.0)	0.080
TKI		11 (15.1)					11 (17.5)	0.0)	
Radiotherapy		17 (23.3)					13 (20.6)	4 (40.0)	
Chemoradiotherapy		6 (8.2)					6 (9.5)	0.0)	
Surgery only		A (5.5)					7 (3.2)	2 (20 0)	

Note: Clinicopathological parameters in the ICI-treated versus ICI-naive/control patients with NSCLC cohort and distribution PDI-PD-L1 interaction status (low versus high patients). Comparisons between groups are Performance statuses are described by means of the WHO guidelines. Bold values indicate statistical significance. on the basis of Fisher's exacts tests, p values are 2-sided.

^aData missing for five ICI-treated patients and 35 ICI-naive control patients.

^bStage at diagnosis/recurrence. ^cData missing for two ICI-naive control patients.

^dData missing for one ICI-treated patient.

AC, adenocarcinoma; chemo, chemotherapy; ICI, immune checkpoint inhibitors; na, not applicable; PD1, programmed cell death protein 1; PD-L1, programmed death ligand 1; SqCC, squamous cell carcinoma; TKl tyrosine kinase inhibitor; TPS, tumor proportion score; WHO, world health organization performed on the basis of Haematoxylin staining with a background radius of 0, a median filter radius of 2, and a sigma value of 1. Nuclei were classified in the range of 8 to 400 μm^2 and expanded by 5 mm to define cells. The threshold for the positive nuclei was set to 0.12 with a maximum background intensity of 2. Example annotations for three classes (positive, negative, and anthracosis) were drawn and were used for training a Random trees (RTress) object classifier, further determining cells as positive or negative.

RNA Extraction

According to availability, a maximum of 5 x 10mm thick FFPE tissue sections from samples of the Sjöberg ICI cohort were used for RNA extraction using the RNeasy FFPE kit (#73504, Qiagen, Hilden, Germany) according to the manufacturer's instructions.

Gene Expression Analysis

For the Uppsala I training cohort, microarray expression data derived from Affymetrix HG U133 Plus 2.0 arrays (54,675 probe sets, Affymetrix) as described previously, ²⁰ was available for 193 patients (accession number GSE37745). For differential gene expression analysis, the 1903 genes included in the gene ontology (GO) term immune response (GO:0006955, biological process) were extracted from the microarray data and analyzed using the limma package (version 3.42.2) with edgeR and Voom extension in R.

For the Sjöberg ICI cohort, the raw RNA sequences were mapped to the GRCh38 human reference genome, and resulting raw counts were used for further analysis (accession number GSE283829). Low-quality samples with overall less than 12,000 detected genes (>10 counts for gene qualification) were ignored for downstream analysis. The analysis of bulk RNAseq samples was performed using R-software (version 4.1.1, R Core Team, Vienna, Austria) and the DESeq2-package (version 1.34.0) with default parameters. For identification of typically overrepresented genes in samples from patients with high PD1-PD-L1 interaction signal (>0.39%) but no response to ICI (graded as stable disease or progressive disease: non-responder), we first performed differentially expressed gene (DEG) analyses comparing samples from non-responders dependent on their PD1-PD-L1 interaction score using a cutoff of greater than or equal to 0.39% (high PLA versus low PLA). Second, we compared samples from all patients with a high interaction score (>0.39%), dependent on their response to immunotherapy (responders versus non-responders). Genes enriched in the high PLA non-responder group from both DEG analyses were selected by log2 fold-change greater than 0.5 and adjusted p value of less than 0.05.

Analysis of Published Single-Cell RNAseq Data Set

Earlier compiled single-cell RNAseq data combining seven data sets from patients with lung cancer was retrieved from the Figshare repository at https://doi.org/10.6084/m9.figshare.c.6222221.v3.²¹ Single-cell raw counts and the accompanying metadata were loaded into R software (version 4.1.1) and processed using the Seurat-package (version 4.3.0). Expression levels of the 13 coenriched genes were visualized using the DotPlot() function. For cell clustering, we utilized the cell type annotation "level2", which identified 27 cell types, as established by the authors. As our genes of interest exhibited low expression across all cancer type annotations, we combined the annotation terms "SOX2 Cancer", "Proliferating Cancer", "LAMC2 Cancer", "CXCL1 Cancer", and "CDKN2A Cancer" into a single "Cancer" term for simplification.

Statistical Analysis

GraphPad Prism (version 10.3.0[461], Boston, MA), Statistical Package for the Social Sciences (version 28.0.1.0, IBM SPSS Statistics, IBM Corp., Armonk, NY), and R software (version 4.3.1) were used for statistical analyses. Correlation analyses between manual and automated marker scoring were performed using Spearman's rank correlations. Intraclass correlation coefficients (two-way random, consistency type) were used to measure the reliability between manual and digital annotations.²³ Contingency tables for the association of marker groups and clinicopathological characteristics were evaluated by chi-square test. Differences between marker groups and immune cell distributions were conducted using the Wilcoxon signed-rank test with Benjamini-Hochberg adjustment for multiple testing. Hierarchical cluster analysis was performed with Euclidean distance and the Ward.D2 method using the pheatmap package (version 1.0.12) for R.

The maxstat package (version 0.7-25) in R was used to determine the maximally selected rank statistics to obtain the best cutoff of the PD1-PD-L1 interaction score with regard to overall survival of ICI-treated patients and to subsequently dichotomize the score into "low" and "high" patient groups. Overall survival analysis since therapy start and within 5 years was undertaken using Kaplan-Meier plots with log rank test and univariable and multivariable Cox regression models with Efron's method for ties and p values based on the Wald test. The assumption of proportional hazards was confirmed through the Schoenfeld residuals test. An interaction term PD1-PD-L1 group (low/high): ICI therapy (no/yes) was included in Cox regression models to assess the relationship between PD1-PD-L1 groups and ICI therapy. All were given 95% confidence intervals (CI) and

statistical tests were two-sided. *P* values of less than 0.05 were considered statistically significant.

Results

The Second-Generation PLA is a Robust Tool to Detect PD1-PD-L1 Interactions in Diagnostic Tissue Samples

To evaluate the reliability of the PLA and the automated digital analysis pipeline, the Uppsala I training cohort TMA consisting of originally 352 patients with surgically treated, ICI treatment-naive NSCLC was stained with the PLA protocol for PD1-PD-L1 interaction (Fig. 1A), and for PD1 and PD-L1 protein by IHC on sequential sections (Fig. 1B). PLA signals were generally observed in tissue regions, which also exhibited PD-L1 and PD1 protein expression (Fig. 1B). Control staining samples for the PLA with only one or no antibody were included, and these displayed no signal (Supplementary Fig. 2A).

Spearman correlations between digital QuPath-based scoring and manual incremental assessment revealed a high interrelationship for all stainings (PD-L1: R = 0.91; PD1: R = 0.88; PLA: R = 0.85 [all p < 0.001]) (Supplementary Fig. 2B). The intraclass correlation coefficients were 0.96 for PD-L1 (95%CI: 0.95–0.97), 0.85 for PD1 (0.69–0.92), and 0.85 for the PLA (0.81–0.89) and indicated excellent to good agreements between digital and manual analyses. Overall, PD-L1 and PD1 protein expression levels within the whole core correlated positively with the frequency of PD1–PD-L1 interactions (adjusted $R^2 = 0.54$, F(2, 294) = 175.9, $p < 2.2e^{-16}$) (Fig. 1C and Supplementary Fig. 2C for individual plots).

Taken together, these data indicate that the second-generation PLA robustly detects PD1-PD-L1 interactions in diagnostic FFPE tissue samples.

PD1-PD-L1 Interaction Marks a Distinct Subset of NSCLC Cases

Patients were further dichotomized into two groups for each respective marker on the basis of the digital annotation of the consecutive tissue sections, using a cutoff of 1% positive cells, in line with clinical PD-L1 assessment (<1% / negative; \ge 1% / positive). Although the expression of both PD1 and PD-L1 was generally required for PLA-positivity, only 104 out of 191 (54.4%) patients positive for both single markers displayed PLA signals in at least 1% of the cells (Fig. 1D). These data suggest that general PD1 and PD-L1 protein levels in single or double marker assays do not warrant PD1-PD-L1 interactions, and thus, the PLA better reflects PD1-PD-L1-mediated immune cell inhibition.

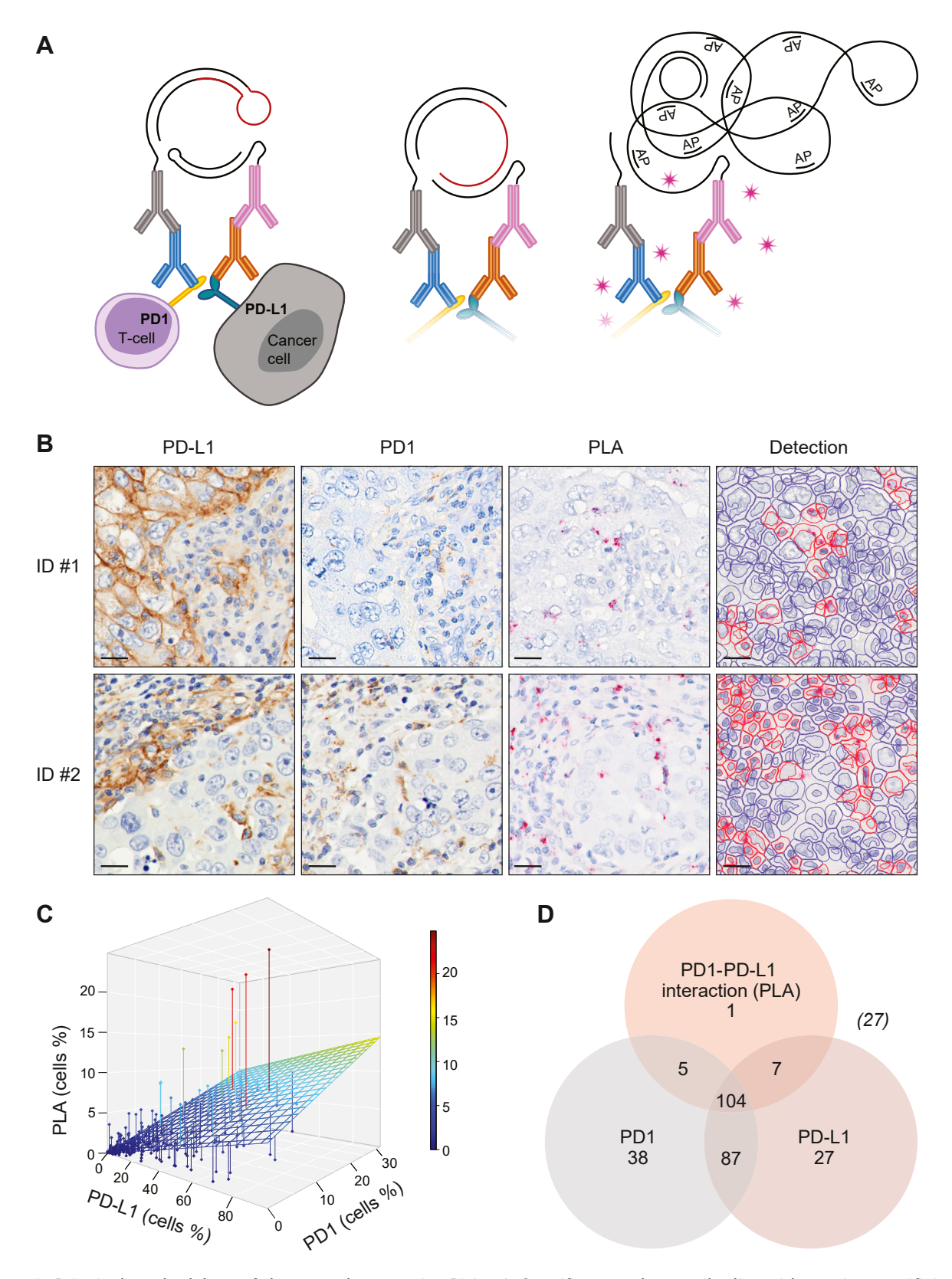


Figure 1. Principal methodology of the second-generation PLA. (A) Specific secondary antibodies with species-specificity for only one of the primary antibodies (anti-PD1/-PD-L1) are conjugated to unique UnFold probes. UnFold probes are enzymatically digested, leading to hybridization of the probes which upon DNA ligation results in a DNA circle. The DNA circle acts as a template for RCA that generates a repetitive single-stranded sequence. Complementary detection oligos conjugated to AP bind to the RCA product. AP produces a red precipitate of FastRed at the site of the PLA reaction. (B) Example images of consecutive sections demonstrating the expression patterns of PD-L1 (left) and PD1 (second from left) investigated with IHC, and their interaction pattern detected with the PLA (second from right) protocol and measured with an automated QuPath pipeline (right) (scale bars = $20~\mu m$). (C) 3D plot illustrating the correlation of the PLA scores to single protein expression levels of PD-L1 and PD1, as assessed by IHC in the Uppsala I training cohort on consecutive sections. Analysis is based on 296

High Levels of PD1-PD-L1 Interaction Coincide With a CD8⁺ T Cell-Rich Yet Exhausted Tumor Phenotype

A high PD1–PD-L1 interaction (PLA) score was associated with an inflamed tumor phenotype with high infiltration of CD4 $^+$, CD8 $^+$, CD3 $^+$, and CD20 $^+$ cells (Spearman R > 0.2, Benjamini-Hochberg adjusted q < 0.001) (Supplementary Fig. 3A). The PD1–PD-L1 interaction had the highest positive correlation with infiltration of CD8 $^+$ cells in the tumor compartment (R = 0.44, q < 0.001).

Notably, EGFR mutations were less frequent among patients with a high PD1-PD-L1 interaction score (p = 0.012, Fisher's exact test) (Supplementary Table 2). No associations were found regarding mutation status for *KRAS* oncogene or *TP53* (Supplementary Fig. 3*A* and Supplementary Table 2).

Differential gene expression analysis on the basis of microarray data restricted to the 1903 genes included in the Gene Ontology Biological Process term immune response (G0:0006955) was performed comparing patients in the upper quarter of the PD1-PD-L1 interaction score versus patients in the lower quarter, resulting in 56 genes differentially expressed (log2 fold-change >0.1 Benjamini-Hochberg adjusted q (Supplementary Fig. 3B and Supplementary Table 3). Cases with high PD1-PD-L1 interaction scores revealed significantly higher expression levels of T cell activation markers (INFG, GZMA, GZMB, GNLY) with simultaneous high expression of markers for T cell exhaustion (CD274/ PDL1, LAG3, IDO1, CTLA4). In summary, high PD1-PD-L1 interaction levels define a subset of patients with NSCLC having high tumoral CD8⁺ T cell infiltration with concurrent immune exhaustion.

Survival analysis stratified by the automated PD1–PD-L1 interaction score using the 1% cutoff did not reveal any survival association (p=0.61, log-rank test) (Supplementary Fig. 3C, left). However, when the best cutoff was chosen, patients with very low PD1–PD-L1 interaction scores ($\leq 0.158\%$) survived shorter than patients with higher scores (p=0.013, log-rank test) (Supplementary Fig. 3C, right). This effect on survival remained significant in univariable Cox regression analysis (HR_{uni} = 0.65 [95%CI: 0.46–0.91], p=0.014) but not in multivariable analysis including the main clinical parameters (HR_{multi} = 0.71 [95%CI: 0.50–1.02], p=0.061) (Supplementary Table 4).

The Level of PD1-PD-L1 Interactions Varies Among Cancer Types and Is Positively Associated With Reported Objective Response Rates to ICI

Pancancer TMAs including 16 different solid tumor types (N = 2 to 15 cases per tumor type) were stained for PD1-PD-L1 interactions and annotated with the automated digital analysis pipeline for the rate of interactions expressed as the percentage of positive cells (Fig. 2A-B). Varying levels of PD1-PD-L1 interactions were found among the different cancer types, with the lowest levels detected in liver cancer (0.02%, SD \pm 0.06%) and the highest in testicular cancer (11.01%, SD \pm 13.93%) (Fig. 2B). Objective response rates to PD1-/ PD-L1 ICI therapies were retrieved for each cancer type from previous reports⁴⁻⁶ and associated with the frequency of PD1-PD-L1 interactions. Tumor types with low interaction levels, such as liver, breast, and gastric cancers, had been previously classified as poor responders to ICI therapies overall. In contrast, cancers with intermediate or high levels, such as melanoma and lung and colorectal cancer, display modest to high response rates. Exceptions, however, were noted for glioblastoma and testicular cancers, which had the highest levels of PD1-PD-L1 interactions, yet presented with low or unknown objective response rates to ICI, respectively (Fig. 2B-C). Although this analysis is based on a few patients, it provides an overview of different cancer types indicating that the levels of PD1-PD-L1 interaction might be associated with benefit from PD1/PD-L1 ICIs.

PD1-PD-L1 Interaction Is a Predictive Marker for Response to PD1/PD-L1 ICI in NSCLC

To assess the response-predictive potential of PD1–PD-L1 interactions with PD1/PD-L1 targeting ICIs, we applied the PLA to the Sjöberg ICI cohort, including 133 patients with advanced-stage NSCLC treated with PD1/PD-L1 ICIs, and control cohort, including 109 ICI-naive patients. FFPE sections of diagnostic biopsies were successfully stained and digitally analyzed for 67 and 73 patients of each cohort, respectively (CONSORT diagram, Supplementary Fig. 1). Significant differences between the ICI-treated patients and the patients without ICI treatment were noted with regard to histological subtype and stage. The control cohort contained no other histological subtypes than adenocarcinomas and squamous cell carcinomas, and more relapsed patients with localized tumors (Table 1).

cases that had information on all three markers available. (D) Venn diagram representing the overlap between the PLA score and PD-L1 and PD1 levels on consecutive sections utilizing a greater than or equal to 1% cutoff for dichotomization of each respective marker into two groups (positive/negative) in the Uppsala I training cohort. A total of 27 patients had a staining frequency of less than 1% for all markers. 3D, three-dimensional; AP, alkaline phosphatase; ID, identification; IHC, immunohistochemistry; PD1, programmed cell death protein 1; PD-L1, programmed death ligand 1; PLA, proximity ligation assay; RCA, rolling circle amplification.

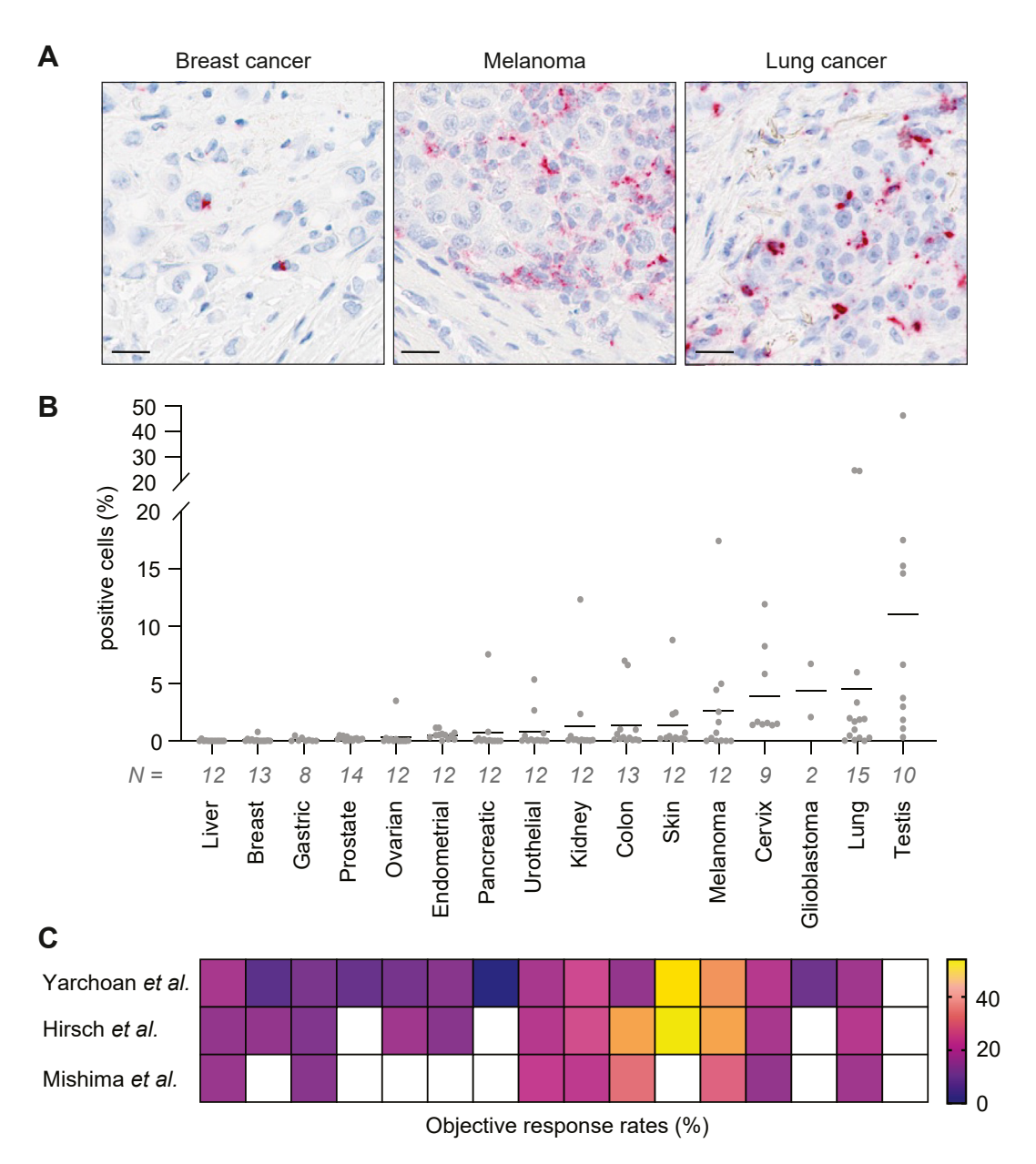


Figure 2. PD1-PD-L1 interaction status across different solid tumor types. (*A*) Example of staining patterns with the PLA protocol in breast cancer, melanoma, and lung cancer. (*B*) Percentage of positive cells for PLA across different solid tumor types. Bars indicate mean values. (*C*) Objective response rates to anti-PD1/anti-PD-L1 ICIs previously reported in other studies for the respective cancer types. ⁴⁻⁶ White boxes are NA. ICI, immune checkpoint inhibitors; IHC, immunohistochemistry; NA, not applicable; PD1, programmed cell death protein 1; PD-L1, programmed death ligand 1; PLA, proximity ligation assay.

Patients were dichotomized into two groups using the best cutoff strategy for survival on the Sjöberg ICI cohort: those with less than 0.39% positive cells were classified as PD1–PD-L1 low (n=36), whereas those with greater than or equal to 0.39% positive cells were classified as PD1–PD-L1 high (n=31). The same cutoff was applied to the ICI-naive control cohort (n=63 PD1–PD-L1 low, n=10 high).

A high PD1-PD-L1 interaction was positively associated with a TPS PD-L1 greater than or equal to 50% in

the ICI-treated patients (p = 0.020, Fisher's exact test). All other clinicopathologic parameters revealed no significant associations in either of the cohorts (Table 1).

In the ICI-treated cohort, patients with a high PLA score exhibited significantly longer survival post-ICI therapy than those with a low PLA score (median survival: 30.9 mo versus 13.5 mo, p=0.010 log-rank test) (Fig. 3A). This was confirmed in a univariate Cox regression model (HR_{uni} = 0.45 [95%CI: 0.24–0.84], p=0.012 Wald test). Notably, in a multivariable Cox

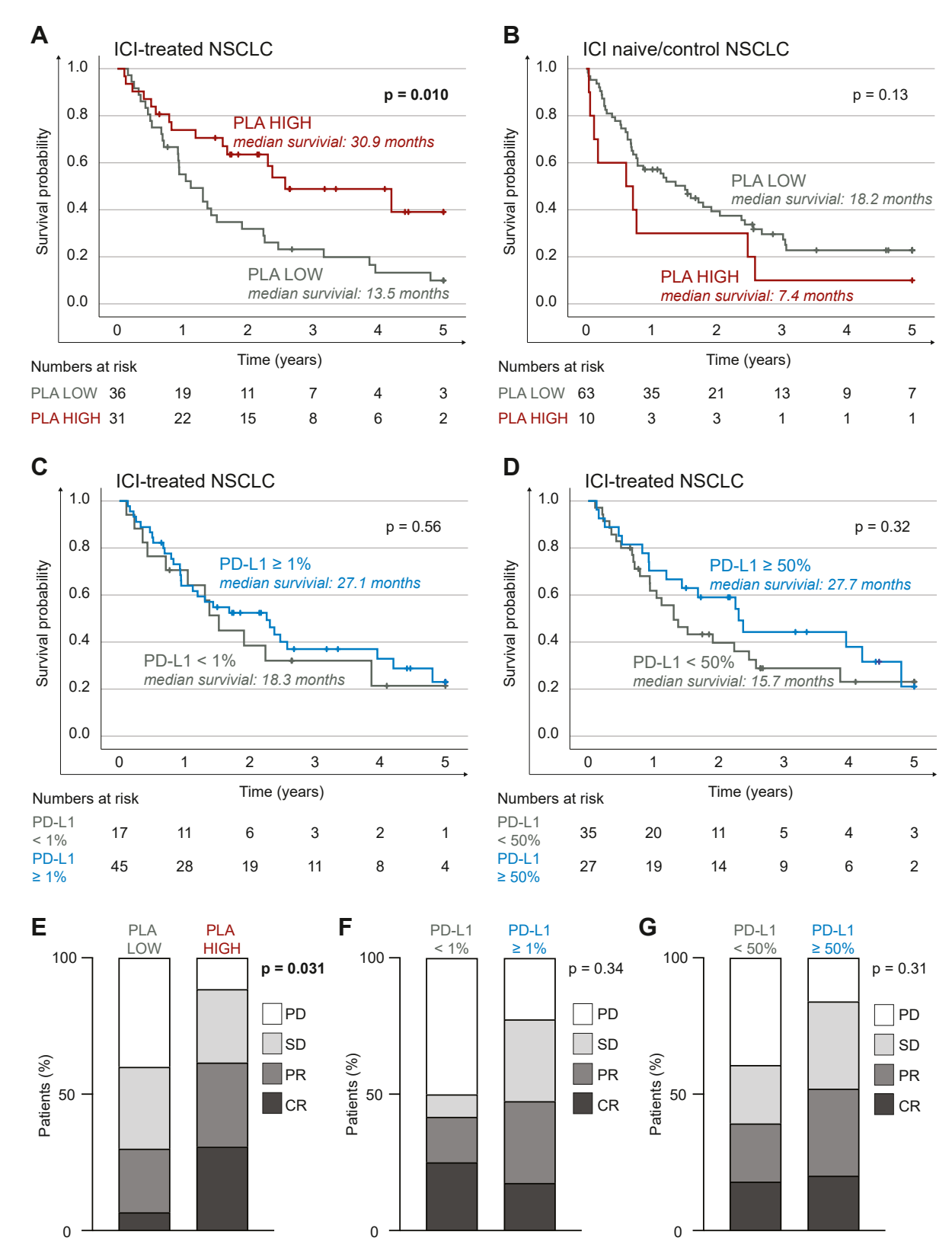


Figure 3. Kaplan-Meier analysis with log-rank test for survival since corresponding therapy initiation truncated at 5 years in dependence of PD1-PD-L1 interaction status (PLA score based on automated pipeline, whole tissue) in (*A*) ICI-treated patients and (*B*) ICI-naive control patients. The cutoff for PD1-PD-L1 interaction was 0.39% positive cells and determined by using the best cutoff strategy on the ICI-treated patients; the same cutoff was applied to the control cohort. (*C*) Kaplan-Meier analysis in dependence on the clinical standard of PD-L1 TPS with a 1% cutoff in ICI-treated patients. (*D*) Kaplan-Meier analysis in dependence of PD-L1 TPS with a 50% cutoff in ICI-treated patients. (*E*) Association between PD1-PD-L1 interaction status and response status. (F+G) Association between PD-L1 TPS and response status. *P* value is on the basis of the chi-square test. CR, complete response; ICI, immune checkpoint inhibitors; IHC, immunohistochemistry; PD, progressive disease; PD1, programmed cell death protein 1; PD-L1, programmed death ligand 1; PLA, proximity ligation assay; PR, partial response; SD, stable disease; TPS, tumor proportion score.

Table 2. Multivariable HR for Death Within 5 Years After Ther	apy Initiation	
ICI-treated patients	HR (95% CI)	p Value
PD1-PD-L1 interaction (LOW/HIGH)	0.45 (0.23-0.89)	0.022
Histological subtype (reference: SqCC)		
AC	0.80 (0.41-1.57)	0.52
Other	0.56 (0.15-2.09)	0.39
Age at diagnosis (<70/> 270 years)	1.41 (0.72-2.73)	0.32
Sex (male/female)	0.84 (0.44-1.58)	0.58
Smoking history (ever-/never-smoker)	1.02 (0.38-2.72)	0.97
Stage (I-III/IV)	0.98 (0.48-1.98)	0.95
ICI-naive/control patients		
PD1-PD-L1 interaction (LOW/HIGH)	1.97 (0.88-4.41)	0.099
Histological subtype (SqCC/AC)	0.46 (0.24-0.91)	0.025
Age at diagnosis (<70/> 270 years)	1.05 (0.59-1.87)	0.87
Sex (male/female)	0.71 (0.40-1.24)	0.23
Smoking history (ever-/never-smoker)	0.81 (0.38-1.73)	0.59
Stage (I-III/IV)	2.11 (1.19-3.73)	0.011
Formal interaction test	,	
PD1-PD-L1 (LOW/HIGH): immunotherapy (crude)	-	0.006
PD1-PD-L1 (LOW/HIGH): immunotherapy (multivariable)	-	0.009
ICI-treated patients		
PD-L1 TPS (<1% / ≥1%)	0.95 (0.46-1.99)	0.89
Histological subtype (reference: SqCC)	,	
AC	1.04 (0.49-2.20)	0.91
Other	0.47 (0.13-1.75)	0.26
Age at diagnosis (<70/> 270 years)	1.40 (0.68-2.90)	0.36
Sex (male/female)	0.70 (0.37-1.34)	0.28
Smoking history (ever-/never-smoker)	1.17 (0.40-3.44)	0.78
Stage (I-III/IV)	1.28 (0.54-3.03)	0.57
ICI-treated patients	,	
PD-L1 TPS (<50% / ≥50%)	0.77 (0.40-1.48)	0.44
Histological subtype (reference: SqCC)	,	
AC	1.02 (0.48-2.15)	0.96
Other	0.51 (0.14-1.90)	0.31
Age at diagnosis (<70/> 270 years)	1.40 (0.70-2.82)	0.35
Sex (male/female)	0.69 (0.36-1.31)	0.26
Smoking history (ever-/never-smoker)	1.15 (0.39-3.37)	0.80
Stage (I-III/IV)	1.34 (0.57-3.12)	0.50

Note: HRs are on the basis of the Cox regression model and *p* values are on the basis of the Wald test. Bold values indicate statistical significance. AC, adenocarcinoma; CI, confidence interval; HR, hazard ratio; ICI, immune checkpoint inhibitors; PD1, programmed cell death protein 1; PD-L1, programmed death ligand 1; SqCC, squamous cell carcinoma; TPS, tumor proportion score.

regression model including histological subtype, age, sex, smoking history, and tumor stage, PD1–PD-L1 interaction remained the only significant variable (high versus low HR_{multi} =0.45 [95%CI: 0.23-0.89], p=0.022) (Table 2). Conversely, analyses of the ICI-naive control cohort revealed no association between PD1–PD-L1 score and survival post therapy initiation (median survival: 7.4 versus 18.2 mo, p=0.13 log-rank test) (Fig. 3B) or risk for death ($HR_{uni}=1.74$ [95%CI: 0.85–3.57], p=0.13 and $HR_{multi}=1.97$ [95%CI: 0.88–4.41], p=0.099) (Table 2).

An interaction term between the PD1-PD-L1 groups (low/high) and ICI treatment status (no/yes) was significant ($p_{crude} = 0.006$; multivariable-adjusted p = 0.006

0.009) (Table 2), indicating that the effect of PD1–PD-L1 interaction is predictive of ICI treatment benefit.

More importantly, PD-L1 TPS of greater than or equal to 1%, currently the clinical standard marker for ICI therapy-eligibility in NSCLC, did not exhibit significant differences in overall survival post-ICI treatment (\geq 1% versus <1% PD-L1 TPS: p=0.56 log-rank test) (Fig. 3C) or the risk of death (HR_{uni} = 0.82 [95%CI: 0.42–1.61], p=0.57; HR_{multi} = 0.95 [0.46–1.99], p=0.89) (Table 2). In addition, a PD-L1 TPS greater than or equal to 50% did not reveal significant differences in survival (\geq 50% versus <50% PD-L1 TPS: p=0.32 log-rank test) (Fig. 3D) or the risk of death (HR_{uni} = 0.73 [0.39–1.37], p=0.33; HR_{multi} = 0.77 [0.40–1.48], p=0.44) (Table 2).

Finally, patients with a high PD1-PD-L1 interaction score experienced more often a partial and complete response to ICI therapy (p=0.031, chi-square test) (Fig. 3E). No association was observed when the diagnostic PD-L1 TPS, with either greater than or equal to 1% or greater than or equal to 50%, was applied (Fig. 3F-G).

Collectively, these findings suggest that the PD1-PD-L1 interaction serves as a superior predictive biomarker for assessing the potential benefit of ICI in patients with NSCLC than PD-L1 TPS.

PD1-PD-L1 Interaction Within the Stromal Compartment Specifically Drives the ICI Response Prediction

To assess whether the spatial location of PD1–PD-L1 interactions is relevant for ICI benefit, a separate annotation of the stromal and tumoral compartments was performed by a board-certified lung pathologist using manual incremental scores. Dichotomization was performed using the best cutoff strategy for each compartment on the ICI-treated patients. The reproducibility of the pathologic annotations was confirmed by a moderate to good agreement with an independent second rater (ICC $_{\rm whole\ biopsy}=0.73$ [95% CI 0.63–0.81], ICC $_{\rm tumor}=0.77$ [0.68–0.84], ICC $_{\rm stroma}=0.65$ [0.51–0.76]) (Supplementary Table 5), reflecting similar concordance as reported for PD-L1 IHC annotations by different pathologists in NSCLC. ^{24,25}

The manual annotation indicated that PD1-PD-L1 interactions were more frequently located within the stroma compartment (Supplementary Fig. 4A-B). In the ICI-treated cohort, high stromal PD1-PD-L1 interaction scores (optimal cutoff point >0%) were associated with significantly longer survival post-ICI therapy than patients with low scores (median survival: 30.9 mo versus 15.7 mo, p = 0.046 log-rank test) (Supplementary Fig. 4C). Univariable Cox regression (high versus low $HR_{uni} = 0.55$ [95%CI: 0.30–1.00], p = 0.050 Wald test), and multivariable analysis (HR_{multi} = 0.50 [95%CI: 0.26– 0.96], p = 0.037) revealed a strong association with prolonged survival (Supplementary Table 6). In contrast, in the ICI-naive control cohort, high PD1-PD-L1 interaction scores were associated with shorter survival (median survival: 8.3 mo versus 18.2 mo, p = 0.043 logrank test) (Supplementary Fig. 4D), confirmed in univariable (high versus low $HR_{uni} = 1.74$ [95%CI: 1.01– 2.99], p = 0.046), but not multivariable Cox regression analysis (Supplementary Table 6).

Regarding PD1–PD-L1 interactions in the tumor compartment (optimal cutoff point >1%), no significant associations with posttreatment survival were found in either cohort (Supplementary Fig. 4E-F); however, the observed survival directions were similar to those in the stroma compartment.

Taken together, these findings confirm the reliability of our assay using different readouts and indicate that stromal PD1-PD-L1 interactions contribute significantly to the predictive impact.

Patients With NSCLC Having High PD1-PD-L1 Interaction Who Do Not Respond to ICI Therapy Exhibit Increased Gene Expression of Other Immune Regulatory Molecules

Although PD1-PD-L1 interaction status was generally predictive of a favorable response to ICI therapy, we observed a subset of patients with PLA-high NSCLC who were defined as non-responders (reported as a stable or progressive disease) (Fig. 3E), indicating treatment resistance. To decipher the molecular characteristics of this patient group, we compared the following: (1) patients with high PD1-PD-L1 interaction levels stratified by their response to ICI (responders versus non-responders), and (2) non-responders to ICI stratified by their PLA interaction status (high PLA versus low PLA) using differential gene expression analysis (Fig. 4A, Supplementary Tables 7-8). We identified 13 genes with significantly increased expression in both comparisons, specifically linking those genes to patients who did not respond to ICI despite high levels of PD1-PD-L1 interaction. Notably, these genes included the chemokines CCL18 and CCL22 and immune regulators (EOMES) and membranous immune checkpoint-associated proteins (HAVCR1 [TIM-1], JAML, and FCRL1) (Fig. 4B-C).

Analysis of a compiled NSCLC single-cell sequencing data set²¹ revealed that these 13 genes were predominantly expressed in specific immune cells, with minimal expression observed in cancer-associated fibroblasts and no detectable expression in cancer cells or endothelial cells (Fig. 4*D*). Particularly high expression levels were observed in monocytes and different subtypes of macrophages, neutrophils, and dendritic cell subsets.

These results reveal the potential role of other stromal immune checkpoint pathways in mediating resistance to ICI therapy and suggest the benefits of combinations of checkpoint inhibitors for therapeutic intervention.

Discussion

Effective PD1/PD-L1 immunotherapy is acting through inhibition of the functional interaction of PD1 and PD-L1, thereby reactivating the immune response. On the basis of this biologic principle, we assessed and validated a second-generation PLA to evaluate the direct interaction of PD1 and PD-L1 within the human cancer microenvironment. Our findings reveal that the PLA effectively identifies a subset of patients with NSCLC having PD1-PD-L1 interactions, a feature not captured

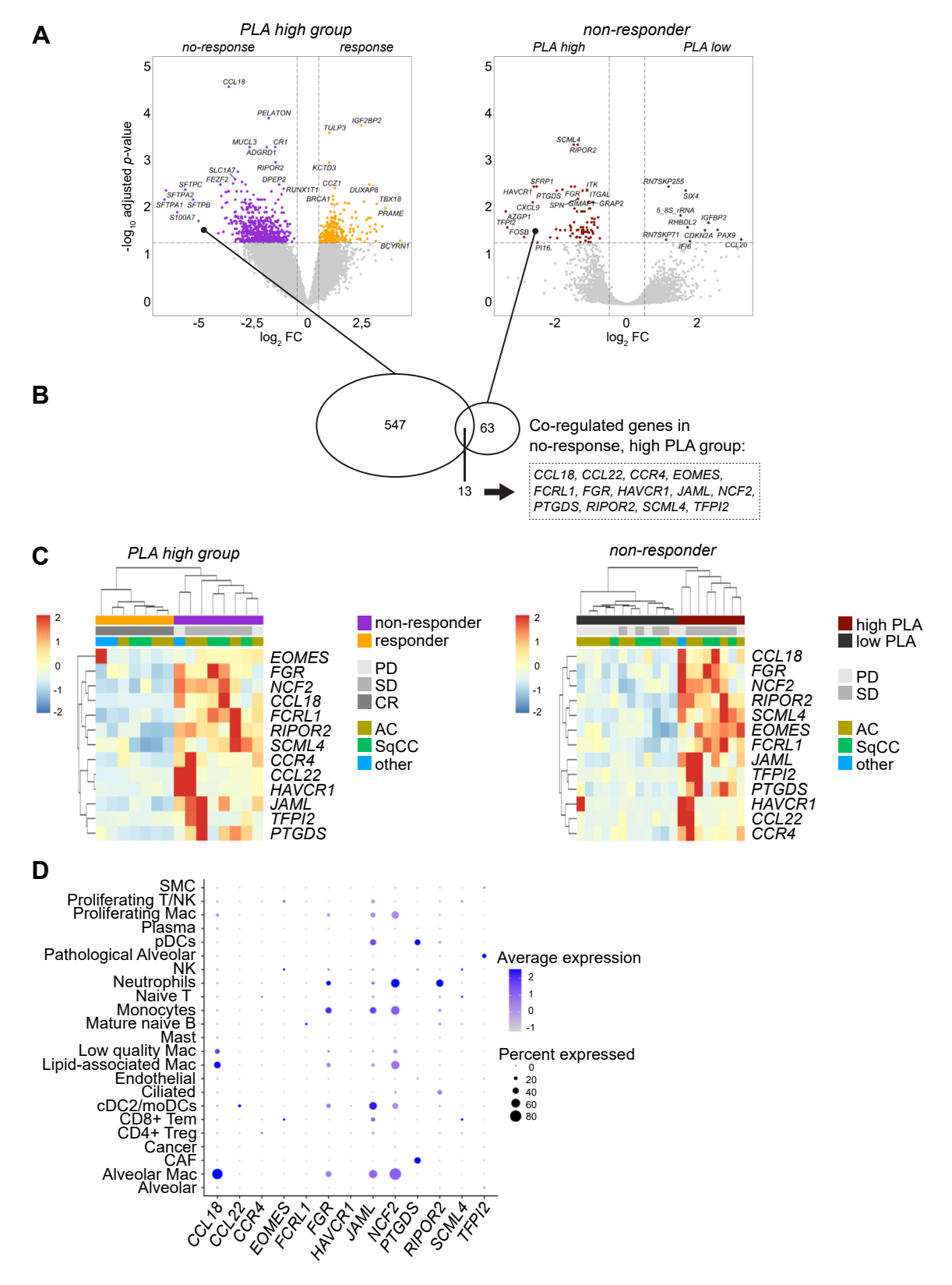


Figure 4. Differential gene expression analysis to identify overrepresented genes in samples from patients with high PD1-PD-L1 interaction scores but no response to immunotherapy treatment (stable disease or progressive disease: non-responder) on the basis of the data from the ICI-treated Sjöberg cohort. (A) Two comparisons were performed: (1) samples from non-responders dependent on their PD1-PD-L1 interaction score with a cutoff of 0.39% (high PLA versus low PLA); (2) all patients with a high PD1-PD-L1 interaction score (\geq 0.39%), dependent on their response to immunotherapy (complete responders versus non-responders). (B) Commonly enriched genes in the high PLA non-responder group from both DEG analyses were selected by log2 fold-change greater than 0.5 and Benjamini-Hochberg adjusted q value less than 0.05. (C) Heatmaps and

by diagnostic IHC for PD1 or PD-L1 proteins alone. This interaction proved to be a strong and independent predictive marker in patients having NSCLC treated with ICI anti-PD1/anti-PD-L1 therapies, associated with radiologic therapy responses and overall survival post therapy initiation. In contrast, no prognostic effect was observed in ICI-naive patients with advanced NSCLC. More importantly, the clinical standard of PD-L1 TPS failed to predict ICI benefit, suggesting that PD1-PD-L1 interaction serves as a superior predictive biomarker to stratify patients with NSCLC to ICI.

The clinical impact of PD1-PD-L1 interaction, predominantly observed in the tumor-adjacent stroma, was related to several important biologic motives that deserve further attention. In agreement with earlier studies of PD-L1-positive tumors, 26,27 cases with high PD1-PD-L1 interaction were associated with a general high immune cell infiltration, particularly high levels of cytotoxic T cells (CD8⁺), indicating an inflamed or "hot" immune phenotype. Our focused analysis of patients with high PD1-PD-L1 interactions but who, nevertheless, did not respond to ICI therapy revealed expression of other immune regulatory elements, including EOMES, FCL1, HAVCR1, and IAML. These alternative immune checkpoint-associated molecules may contribute functionally to ICI therapeutic efficacy or resistance, and could potentially be targeted with agonistic or blocking antibodies in efforts to develop combination therapies. There are already indications in the literature that some of these molecules play a role in immune responses to tumors. Antibodies to the costimulatory molecule JAML, expressed in tumorinfiltrating and tissue-resident T cells and also in natural killer cells, were reported to act synergistically with ICI treatment in murine melanoma models. 28,29 Similarly, there is evidence in support of the role of TIM-1/HAVCR1 expressed by B cells in the regulation of intratumoral inflammation.³⁰ This observed immune state might reflect a specific T cell exhaustion phenotype, distinct from the dysfunctional T cell phenotype, as it has the potential to be reverted to an effector function. We emphasize that validating these findings in larger, independent cohorts and conducting functional analyses will be crucial to pinpoint the immune regulatory mechanisms underlying resistance to immune checkpoint inhibition. Nevertheless, our results underscore the value of a detailed diagnostic tool for assessing the functional states of PD1-PD-L1 interactions. They also suggest a potential future framework to incorporate this approach with other checkpoint molecules, enabling therapeutic strategies that combine stimulatory and inhibitory interventions to overcome resistance. 31,32

The assumption that PD-L1 expression alone is insufficient to determine the efficacy of ICIs is not novel, as evidenced by efforts to incorporate further immune markers in predictive gene signatures or spatial prediction scores in different cancer types. 33-36 However, only two studies directly addressed the spatial relation of PD1-PD-L1 relationship in the context of ICIs in lung cancer. Gavrielatou et al.¹³ used a multiplex immunofluorescent approach applying overlapping channels to establish a co-localization score that was associated with therapy response, progression-free survival, and overall survival in ICI-treated patients with NSCLC. In the multicenter study of Sánchez-Magraner et al, 14 the complex Förster resonance energy transfer technique was used to detect receptor-ligand interactions. Yet again, high interaction metrics better predicted survival than the IHC PD-L1 score alone. Our study corroborates these results and, in addition, provides evidence that the PD1-PD-L1 interaction phenotype is primarily not of prognostic value in advanced-stage NSCLC (formal interaction test) and independent from main clinical parameters (multivariate analysis). More importantly, here, we present the essential technical advancement that enables the transfer of this critical spatial information into clinical diagnostics. The PLA technique qualifies as a diagnostic tool, because: (1) it is applicable to a single tissue section of FFPE patient biopsies, (2) does not require specialized equipment, (3) can be easily standardized across different diagnostic centers, and (4) can be evaluated under the bright field microscopy either classically by a pathologist or with a digital approach. Thus, the PLA is an ideal prospect for the development of a companion diagnostic test to stratify patients with cancer for ICI.

Indeed, our pancancer analyses revealed that PD1-PD-L1 interactions generally occur in cancer types sensitive to PD1/PD-L1 blockade. This finding is relevant for cancer types in which currently no reliable biomarkers exist, for example, in melanoma, or those with evaluation systems of limited value and poor producibility such as cervical cancer. This finding is albeit on the basis of a limited number of patients and presented with high interpatient variability and should be addressed further in future studies.

A notable strength of our study was the use of realworld diagnostic pretreatment biopsies reflecting the current diagnostic workflow in clinical routine. However, although the data is motivating, some limitations of our study should be considered. The patients of the Sjöberg

cluster analysis illustrate the differentially expressed genes within the study groups. (*D*) Cellular expression pattern of the differentially expressed genes on the basis of analysis of a publicly available integrated NSCLC single-cell data set with cell subtype annotation (level 2).²¹ AC, adenocarcinoma; CR, complete response; DEG, differentially expressed gene; FC, fold change; PD, progressive disease; PD1, programmed cell death protein 1; PD-L1, programmed death ligand 1; PLA, proximity ligation assay; SD, stable disease; SqCC, squamous cell carcinoma.

ICI study cohort received heterogeneous treatment schemes—varying numbers of cycles, in different lines of treatment, and monotherapy versus combinatory modalities. We were also unable to fully match the immunotherapy cohort with an ICI-naive control cohort. There were differences in primary stages and histological subtype, potentially confounding the assessments of PD1-PD-L1 interaction as a predictor of ICI benefit. Because of the retrospective nature of our cohort, treatment decisions influenced by PD-L1 TPS scores may have resulted in a lower number of patients with high PD1-PDL1 interaction levels in the ICI-naive/control group. In addition, we could not fully align our radiologic response data with the immunotherapy Response Evaluation Criteria in Solid Tumors criteria, because computed tomography or magnetic resonance imaging during follow-up were inconsistently applied on the basis of the individual decision of the treating clinician. All these challenges are inherent in retrospective studies and can only be addressed in a prospective, randomized setting, in the optimal scenario with a head-to-head comparison and stratification of the PD-L1 TPS against the PD1-PD-L1 interaction score.

Taken together, numerous studies have reported the poor performance of the current stratification standard using PD-L1 tumor expression. Our results, along with findings from other studies, strongly suggest that functional PD1-PD-L1 interaction is a superior read-out for predicting ICI benefit. Therefore, the operative PD1-PD-L1 PLA, which provides this critical functional information on PD1-PD-L1 interaction, presents a fundamentally new concept to advance precision diagnostic to the next necessary level. Integrating this assay into routine clinical diagnostics is feasible, allowing for interpretation by means of semiquantitative assessment by a pathologist or automated image analysis. However, it requires further validation and pathologist training for scoring harmonization.

CRediT Authorship Contribution Statement

Conceptualization – A.L, P.M, C.S. Methodology – A.L, P.M, C.S. Software – A.L, L.M, C.S. Validation – A.L, R.A, P.M, C.S. Formal analysis – A.L, L.M, R.A, L.H, H.Y, M.B, A.M. Investigation – A.L, L.H, R.A. Resources – C.L, J.B, J.I, P.M, C.S. Data curation – A.L, J.F, J.M, L.M, N.H, J.B, E.B, J.I, M.G, P.M. Writing: Original draft – A.L, L.M, P.M, C.S. Writing: Review & Editing – A.L, J.M, L.H, L.M, H.B, K.K, P.M, C.S. Visualization – A.L, L.H, L.M, P.M, C.S. Supervision – A.L, P.M, C.S. Project Administration – P.M, C.S. Funding Acquisition – P.M, C.S.

Disclosure

Dr. Botling received grants to institution from Amgen and Bristol-Myers Squibb and received personal

honoraria from Astra Zeneca, Merck Sharp & Dohme, Roche, Pfizer, Bristol-Myers Squibb, Boehringer-Ingelheim, Novartis, GSK, Lilly, Amgen, Incyte, Daiichi, and Sanofi. Dr. Kärre received personal honoraria from Segulah Medical Acceleration and Anocca AB and is pro bono secretary general at the European Academy for Cancer Sciences and received travel support from them. Dr. Isaksson is a scientific board member and received honoraria for lectures from Amgen, Astra Zeneca, Bristol-Myers Squibb, Merck Sharp & Dohme, and Roche; and is a pro bono committee member of the Swedish Lung Cancer Study Group. Dr. Strell received research reagents (to institution) from Navinci Diagnostics AB. The remaining authors declare no conflict of interest.

Acknowledgments

This study received funding through the following authors: Dr. Strell from the Norwegian Cancer Society (#255690), the Swedish Cancer Society (21149PJ), The Swedish Research Council (2022-01151), and a starting grant from Trond Mohn Foundation (TMS2022STG01); Dr. Micke from the Sjöberg Foundation, The Swedish Cancer Society (211790PJ), The Swedish Research Council (2021-02693), and The Lions Cancer Foundation Uppsala; Dr. Isaksson from the Gävle Cancer Society; Dr. Kärre from the Sjöberg Foundation and the Swedish Cancer Society (201368Pj); and Ms. Lindberg from the Dr. Margaretha Nilsson Stiftelse for Medicinsk Forskning (travel grant). The authors also thank the Research, Development, and Teaching Unit at the Department of Clinical Pathology of Uppsala University Hospital, Uppsala, Sweden, for practical support.

Supplementary Data

Note: To access the supplementary material accompanying this article, visit the online version of the *Journal of Thoracic Oncology* at www.jto.org and at https://doi.org/10.1016/j.jtho.2024.12.026.

References

- Bagchi S, Yuan R, Engleman EG. Immune checkpoint inhibitors for the treatment of cancer: clinical impact and mechanisms of response and resistance. Annu Rev Pathol. 2021;16:223-249.
- Antonia SJ, Borghaei H, Ramalingam SS, et al. Four-year survival with nivolumab in patients with previously treated advanced non-small-cell lung cancer: a pooled analysis. *Lancet Oncol*. 2019;20:1395-1408.
- Garon EB, Rizvi NA, Hui R, et al. Pembrolizumab for the treatment of non-small-cell lung cancer. N Engl J Med. 2015;372:2018-2028.
- Yarchoan M, Hopkins A, Jaffee EM. Tumor mutational burden and response rate to PD-1 inhibition. N Engl J Med. 2017;377:2500-2501.

- 5. Hirsch L, Zitvogel L, Eggermont A, Marabelle A. PD-Loma: a cancer entity with a shared sensitivity to the PD-1/PD-L1 pathway blockade. *Br J Cancer*. 2019;120:3-5.
- Mishima S, Taniguchi H, Akagi K, et al. Japan Society of Clinical Oncology provisional clinical opinion for the diagnosis and use of immunotherapy in patients with deficient DNA mismatch repair tumors, cooperated by Japanese Society of Medical Oncology, First Edition. *Int J Clin Oncol*. 2020;25:217-239.
- Suijkerbuijk KPM, Van Eijs MJM, Van Wijk F, Eggermont AMM. Clinical and translational attributes of immune-related adverse events. Nat Cancer. 2024;5:557-571.
- Zaim R, Redekop K, Uyl-de Groot CA. Immune checkpoint inhibitors for the treatment of non-small cell lung cancer: a comparison of the regulatory approvals in Europe and the United States. *J Cancer Policy*. 2022;33:100346.
- 9. De Castro G Jr, Kudaba I, Wu YL, et al. Five-year outcomes with pembrolizumab versus chemotherapy as first-line therapy in patients with non-small-cell lung cancer and programmed death ligand-1 tumor proportion score ≥ 1% in the KEYNOTE-042 study. *J Clin Oncol*. 2023;41:1986-1991.
- Socinski MA, Nishio M, Jotte RM, et al. IMpower150 final overall survival analyses for atezolizumab Plus bevacizumab and chemotherapy in first-line metastatic nonsquamous NSCLC. J Thorac Oncol. 2021;16:1909-1924
- Hellmann MD, Paz-Ares L, Bernabe Caro R, et al. Nivolumab plus ipilimumab in advanced non-small-cell lung cancer. N Engl J Med. 2019;381:2020-2031.
- 12. Perrone F, Leonetti A, Tiseo M, Facchinetti F. Benefit with no target: long-term outcomes of chemo-immunotherapy in "PD-L1 negative" NSCLC. *J Thorac Oncol*. 2024;19:1128-1132.
- 13. Gavrielatou N, Liu Y, Vathiotis I, et al. Association of PD-1/PD-L1 co-location with immunotherapy outcomes in non-small cell lung cancer. *Clin Cancer Res*. 2022;28:360-367.
- 14. Sánchez-Magraner L, Gumuzio J, Miles J, et al. Functional engagement of the PD-1/PD-L1 complex But not PD-L1 expression is highly predictive of patient response to immunotherapy in non-small-cell lung cancer. *J Clin Oncol*. 2023;41:2561-2570.
- **15.** Klaesson A, Grannas K, Ebai T, et al. Improved efficiency of in situ protein analysis by proximity ligation using UnFold probes. *Sci Rep.* 2018;8:5400.
- **16.** Edlund K, Lindskog C, Saito A, et al. CD99 is a novel prognostic stromal marker in non-small cell lung cancer. *Int J Cancer*. 2012;131:2264-2273.
- 17. Edlund K, Madjar K, Mattsson JSM, et al. Prognostic impact of tumor cell programmed death ligand 1 expression and immune cell infiltration in NSCLC. *J Thorac Oncol*. 2019;14:628-640.
- **18.** Goldmann T, Marwitz S, Nitschkowski D, et al. PD-L1 amplification is associated with an immune cell rich phenotype in squamous cell cancer of the lung. *Cancer Immunol Immunother*. 2021;70:2577-2587.

- **19.** Bankhead P, Loughrey MB, Fernández JA, et al. QuPath: open source software for digital pathology image analysis. *Sci Rep.* 2017;7:16878.
- 20. Micke P, Edlund K, Holmberg L, et al. Gene copy number aberrations are associated with survival in histologic subgroups of non-small cell lung cancer. *J Thorac Oncol*. 2011;6:1833-1840.
- 21. Prazanowska KH, Lim SB. An integrated single-cell transcriptomic dataset for non-small cell lung cancer. *Sci Data*. 2023;10:167.
- 22. Hao Y, Hao S, Andersen-Nissen E, et al. Integrated analysis of multimodal single-cell data. *Cell*. 2021;184:3573-3587.e29.
- 23. Koo TK, Li MY. A guideline of selecting and reporting intraclass correlation coefficients for reliability research. *J Chiropr Med*. 2016;15:155-163.
- 24. Brunnström H, Johansson A, Westbom-Fremer S, et al. PD-L1 immunohistochemistry in clinical diagnostics of lung cancer: inter-pathologist variability is higher than assay variability. *Mod Pathol*. 2017;30:1411-1421.
- **25.** Troncone G, Gridelli C. The reproducibility of PD-L1 scoring in lung cancer: can the pathologists do better? *Transl Lung Cancer Res.* 2017;6:S74-S77.
- **26.** Taube JM, Klein A, Brahmer JR, et al. Association of PD-1, PD-1 ligands, and other features of the tumor immune microenvironment with response to anti-PD-1 therapy. *Clin Cancer Res.* 2014;20:5064-5074.
- 27. Backman M, La Fleur L, Kurppa P, et al. Infiltration of NK and plasma cells is associated with a distinct immune subset in non-small cell lung cancer. *J Pathol*. 2021;255:243-256.
- 28. McGraw JM, Thelen F, Hampton EN, et al. JAML promotes CD8 and $\gamma\delta$ T cell antitumor immunity and is a novel target for cancer immunotherapy. *J Exp Med*. 2021;218: e20202644.
- 29. Eschweiler S, Wang A, Ramírez-Suástegui C, et al. JAML immunotherapy targets recently activated tumorinfiltrating CD8+ T cells. *Cell Rep.* 2023;42:112040.
- **30.** Bod L, Kye YC, Shi J, et al. B-cell-specific checkpoint molecules that regulate anti-tumour immunity. *Nature*. 2023;619:348-356.
- 31. Kagamu H. Immunotherapy for non-small cell lung cancer. *Respir Investig*. 2024;62:307-312.
- 32. Blank CU, Haining WN, Held W, et al. Defining 'T cell exhaustion'. *Nat Rev Immunol*. 2019;19:665-674.
- 33. Aung TN, Warrell J, Martinez-Morilla S, et al. Spatially informed gene signatures for response to immunotherapy in melanoma. *Clin Cancer Res.* 2024;30:3520-3532.
- Gil-Jimenez A, Van Dijk N, Vos JL, et al. Spatial relationships in the urothelial and head and neck tumor microenvironment predict response to combination immune checkpoint inhibitors. Nat Commun. 2024;15:2538.
- **35.** Wang XQ, Danenberg E, Huang CS, et al. Spatial predictors of immunotherapy response in triple-negative breast cancer. *Nature*. 2023;621:868-876.
- 36. Yang Q, Gong H, Liu J, Ye M, Zou W, Li H. A 13-gene signature to predict the prognosis and immunotherapy responses of lung squamous cell carcinoma. *Sci Rep.* 2022;12:13646.